

Transfer Learning in Quantum Parametric Classifiers: An Information-Theoretic Generalization Analysis

Sharu Theresa Jose and Osvaldo Simeone

Abstract—A key step in quantum machine learning with classical inputs is the design of an embedding circuit mapping inputs to a quantum state. This paper studies a transfer learning setting in which classical-to-quantum embedding is carried out by an arbitrary parametric quantum circuit that is pre-trained based on data from a source task. At run time, the binary classifier is then optimized based on data from the target task of interest. Using an information-theoretic approach, we demonstrate that the average excess risk, or optimality gap, can be bounded in terms of two Rényi mutual information terms between classical input and quantum embedding under source and target tasks, as well as in terms of a measure of similarity between the source and target tasks related to the trace distance. The main theoretical results are validated on a simple binary classification example.

I. INTRODUCTION

Parametric quantum circuits (PQCs) have emerged as a viable solution to leverage noisy intermediate-scale quantum (NISQ) quantum processors [1]. A PQC is a quantum circuit that produces a quantum output state via a sequence of quantum gates that may depend on input data x and model parameter vector θ . Unlike more traditional, but currently less practical, fault-tolerant quantum computing routines, PQCs are not handcrafted assuming noiseless quantum gates, but they are rather optimized – through the parameter vector θ – by using a classical optimization strategy that minimizes the expectation of an observable of the output state.

A key step in quantum machine learning with classical inputs is the design of an embedding circuit mapping inputs to a quantum state [1, Chap. 6]. This is illustrated in Fig. 1, in which the classical input vector x is mapped, via a PQC with a given ansatz, to a quantum state defined by a density matrix $\rho_\theta(x)$. We are interested in the task of classifying the input x by applying a quantum measurement to the density matrix $\rho_\theta(x)$ [1], [2]. Since the (classical) ground-truth distribution $p^T(c, x)$ describing the correlation between label c and input x for the *target task* of interest is assumed to be unknown, the classifying quantum measurement is optimized based on supervised examples of the form (c, x) drawn from distribution $p^T(c, x)$. Reference [3] has recently studied the generalization properties of the circuit in Fig. 1 for a *fixed* embedding

The authors are with the King’s Communications, Learning, and Information Processing Lab of the Department of Engineering, King’s College London, WC2R 2LS (emails: sharu.jose@kcl.ac.uk, osvaldo.simeone@kcl.ac.uk). They have received funding from the European Research Council (ERC) under the European Union’s Horizon 2020 Research and Innovation Programme (Grant Agreement No. 725731). The authors would like to thank Dr. Ivana Nikoloska for useful discussions in the early stages of this work.

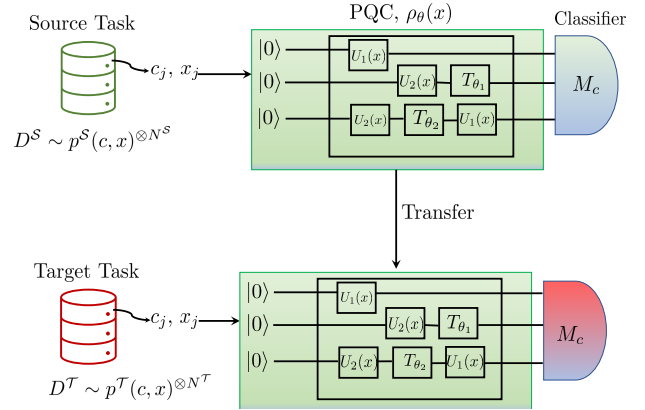


Fig. 1: Illustration of the transfer learning problem under study. Data from the source task (green) is used to learn the parameters θ of the parameterized quantum circuit (PQC) implementing classical-to-quantum embedding which is then fixed for use by the target task. The target task uses its data (red) to learn the optimal task-specific binary classifier.

parameter θ as a function of the number of examples N^T from an information-theoretic viewpoint. The authors show that the excess risk, or optimality gap, can be bounded as $O(\sqrt{2I_2^T(X; R_\theta)}/\sqrt{N^T})$, where $I_2^T(X; R_\theta)$ is the 2-Rényi mutual information (MI) between the classical input x and the quantum representation $\rho_\theta(x)$ under the classical-quantum state $\rho_{XR} = \mathbb{E}_{p^T(x)}[|x\rangle\langle x| \otimes \rho_\theta(x)]$, with $p^T(x)$ being the marginal of $p^T(c, x)$ [4].

In this paper, we consider the practical case in which one needs to design *both* embedding and classifying measurement, while having access only to limited data from the target task. To address this problem, following [5], we assume that the embedding circuit producing the state $\rho_\theta(x)$ is *pre-trained* based on, generally more numerous, data from a related *source task* with underlying distribution $p^S(c, x)$. Once the embedding circuit is fixed, data from the target task is used only to adapt the classifying measurement as in [3]. Extending the analysis in [3], we prove that the average excess risk can be bounded in terms of (i) the 2-Rényi MIs between classical input and quantum embedding under source and target tasks; (ii) the Rademacher complexity of the cascade of circuit and measurement under the source task, which depends on the specific ansatz of the PQC [6]–[8]; and (iii) a specific measure of (dis)similarity between the source and target tasks.

Overall, this work contributes to the body of research on information-theoretic aspects of quantum statistical signal processing (see, e.g., [9] for recent results), and presents a new characterization of similarity between the tasks that facilitate quantum transfer learning. Apart from the mentioned reference [3], the generalization properties of a quantum circuit was studied via an information geometric approach based on Fisher information in [10]. Also related is reference [11], which studies a classical version of the problem considered in this work, revealing the role of task similarity for transfer representation learning.

II. PROBLEM FORMULATION

In this section, we first describe the quantum classification problem studied in [3] for a fixed quantum embedding parameter vector θ ; and then present the two-stage transfer learning problem illustrated in Fig. 1 in which the embedding circuit parameter θ is pre-trained based on data from a source task.

A. Quantum Classification with a Fixed Embedding

Let x denote the classical input feature vector and $c \in \{0, 1\}$ be the corresponding class index, which identifies one of two possible classes. We take x to assume values in an arbitrary discrete finite set. The data sample (c, x) is generated from an *unknown* underlying joint distribution $p^T(c, x)$ describing the *target* task. The *embedding circuit* maps the classical feature vector x to a density matrix $\rho_\theta(x) \geq 0$, a positive semi-definite unit-trace matrix defined on some (finite-dimensional) Hilbert space. The embedding circuit is implemented by a PQC parameterized by a (classical) parameter vector $\theta \in \Theta$, where Θ is an arbitrary set.

The *classifier* consists of a positive operator-valued measure (POVM) applied to the quantum state $\rho_\theta(x)$. The POVM is defined by the set of positive-semidefinite matrices $M = \{M_c\}_{c=0}^1$, of the same dimensions of the density matrix $\rho_\theta(x)$, that satisfy the conditions $M_c \geq 0$ and $\sum_{c=0}^1 M_c = I$. By Born's rule, the classifier chooses class c with probability $\text{Tr}(M_c \rho_\theta(x))$, where $\text{Tr}(\cdot)$ represents the trace operation. We use $\mathcal{M} = \{M : M_c \geq 0, \sum_{c=0}^1 M_c = I\}$ to denote the set of all POVMs.

For a fixed embedding parameter θ , quantum supervised classification [3] optimizes the POVM $M \in \mathcal{M}$ with the ideal goal of minimizing the expected probability of error, also known as *expected risk*,

$$\mathcal{R}_{\theta, M}^T = \mathbb{E}_{p^T(c, x)}[\ell_{\theta, M}(c, x)] \quad (1)$$

over $M \in \mathcal{M}$, where

$$\ell_{\theta, M}(c, x) = 1 - \text{Tr}(M_c \rho_\theta(x)) \quad (2)$$

is the probability of error evaluated on an example (c, x) . Since the ground-truth joint distribution $p^T(c, x)$ is unknown, the optimization of the POVM M is done using a training data set $\mathcal{D}^T = \{(c_1, x_1), \dots, (c_{N^T}, x_{N^T})\}$ of N^T samples, whose individual data points (c_j, x_j) are assumed to be independent

identically distributed (i.i.d.) according to $p^T(c, x)$. Specifically, the POVM is obtained by minimizing the *empirical training loss*

$$\widehat{\mathcal{R}}_{\theta, M}^T = \frac{1}{N^T} \sum_{(c, x) \in \mathcal{D}^T} \ell_{\theta, M}(c, x). \quad (3)$$

The solution of this optimization can be obtained in closed form for binary classification yielding the so-called *Hellstrom measurement* (see [2, Sec. III]). We write as

$$\widehat{M}_\theta^T = \arg \min_{M \in \mathcal{M}} \widehat{\mathcal{R}}_{\theta, M}^T \text{ and } \widehat{\mathcal{R}}_\theta^T = \widehat{\mathcal{R}}_{\theta, \widehat{M}_\theta^T}^T \quad (4)$$

the corresponding optimal POVM and the minimized expected risk for a fixed θ , respectively.

The classifier obtained with the resulting POVM is said to generalize well if it yields a low expected risk (2). In this regard, a key metric of interest is the *excess risk*

$$\Delta \mathcal{R}_\theta^T = \mathcal{R}_{\theta, \widehat{M}_\theta^T}^T - \min_M \mathcal{R}_{\theta, M}^T, \quad (5)$$

which is the difference between the expected risk (1) obtained via the outlined learning process and the genie-aided expected risk obtained with the optimal POVM. An information-theoretic bound on the excess risk (5) was derived in [3] for a fixed parameter θ .

B. Transfer Learning for Quantum Classification

In this work, as illustrated in Fig. 1, we consider a two-stage transfer learning problem, in which the embedding parameter vector θ is pre-trained based on data from a *source* task with underlying true data distribution $p^S(c, x)$, which is generally different from the distribution $p^T(c, x)$ of the target task. To this end, we assume to have access to a training set $\mathcal{D}^S = \{(c_1, x_1), \dots, (c_{N^S}, x_{N^S})\}$ of N^S samples generated i.i.d. according to the source task distribution $p^S(c, x)$. In a typical implementation, one may have a number of data samples N^S from the source task that is larger than for the target task, i.e., $N^T \ll N^S$, although we will not need this assumption in the following. In the first phase of the transfer learning process, the source-task data set \mathcal{D}^S is used to optimize the embedding parameter θ , along with the classifying measurement, i.e., the POVM, for the source task. In the second phase, the embedding parameter is fixed to the pre-trained value $\hat{\theta}$ obtained from the first phase, and the POVM for the target task is optimized as described in the previous subsection.

To elaborate, in the *first phase*, the embedding parameter vector θ is obtained by minimizing the empirical training loss on the source-task data, i.e.,

$$\hat{\theta} = \arg \min_{\theta \in \Theta} \min_{M \in \mathcal{M}} \widehat{\mathcal{R}}_{\theta, M}^S = \arg \min_{\theta \in \Theta} \widehat{\mathcal{R}}_\theta^S, \quad (6)$$

where we have defined the source-task empirical training loss as $\widehat{\mathcal{R}}_{\theta, M}^S = \sum_{(c, x) \in \mathcal{D}^S} \ell_{\theta, M}(c, x) / N^S$ (cf. (3)), and we have used a notation analogous to (4). In the *second stage*, the classifying measurement is optimized as in (4) using the target-task data for a fixed embedding parameter vector (6), yielding the POVM \widehat{M}_θ^T and the expected risk $\widehat{\mathcal{R}}_\theta^T = \widehat{\mathcal{R}}_{\theta, \widehat{M}_\theta^T}^T$.

In order to evaluate the generalization properties of transfer learning, we adopt the *transfer excess risk*

$$\Delta \mathcal{R}^{\mathcal{S} \rightarrow \mathcal{T}} = \mathcal{R}_{\hat{\theta}, \hat{M}_{\hat{\theta}}}^{\mathcal{T}} - \min_{\theta \in \Theta, M \in \mathcal{M}} \mathcal{R}_{\theta, M}^{\mathcal{T}}. \quad (7)$$

Unlike the excess risk in (5), the transfer excess risk captures the impact on generalization not only of the classifier (trained using target-task data), but also of the embedding parameter θ (pre-trained using source-task data).

III. TRANSFER EXCESS RISK FOR BINARY QUANTUM CLASSIFICATION

In this section, we present our main result – a high-probability bound on the transfer excess risk for binary quantum classification. Towards this goal, we start with some preliminary background on quantum information and measures, and then define a useful notion of similarity between source and target tasks, which is finally leveraged to describe the derived bound on the transfer excess risk in terms of Rényi mutual information.

A. Preliminaries

Let ρ and σ denote two positive semi-definite matrices defined on the same (finite-dimensional) Hilbert space. The *trace distance* $T(\rho, \sigma)$ between the matrices is the counterpart of the total variation for probability distributions [4], [12], and it can be written as

$$T(\rho, \sigma) = \frac{1}{2} \|\rho - \sigma\|_1 = \frac{1}{2} \text{Tr}(|\rho - \sigma|), \quad (8)$$

where $\text{Tr}(|A|)$, with $|A| = (A^\dagger A)^{1/2}$ being the positive semi-definite square root of the Hermitian matrix A , is the *trace norm* of matrix A , and A^\dagger denotes the conjugate transpose of A . The trace distance is bounded as $0 \leq T(\rho, \sigma) \leq 1$ and satisfies the triangle inequality [4], [12].

Consider a bipartite quantum system consisting of quantum subsystems A and B with the joint density matrix ρ_{AB} . For any real number $\alpha \neq 1$, the α -*Rényi mutual information (MI)* between the subsystems A and B is defined as [13]

$$I_\alpha(A; B) = \frac{\alpha}{\alpha - 1} \log_2 \text{Tr} \left(\text{Tr}_A \left(\rho_A^{(1-\alpha)/2} \rho_{AB}^\alpha \rho_A^{(1-\alpha)/2} \right) \right)^{\frac{1}{\alpha}}, \quad (9)$$

where $\rho_A = \text{Tr}_B(\rho_{AB})$ is the reduced density matrix for the subsystem A obtained by tracing out system B via the partial trace (i.e., marginalization) operation $\text{Tr}_B(\cdot)$. For $\alpha \rightarrow 1$, one recovers the quantum mutual information $I(A : B) = H(A) + H(B) - H(AB)$, where $H(A) = S(\rho_A) = -\text{Tr}(\rho_A \log \rho_A)$ is the von Neumann entropy for system A and similar definitions apply to the other entropy terms.

B. On the Similarity of Source and Target Tasks

The generalization performance of transfer learning depends intuitively on how similar the embedding parameter vectors θ that minimize the losses on the source and target tasks are. Based on this intuition, this subsection develops a notion of (dis)similarity between source and target tasks, which is

central to the bound on the transfer excess risk presented in the next subsection.

Let

$$\rho_{\theta, c}^A = \mathbb{E}_{p^{\mathcal{A}}(x|c)}[\rho_\theta(x)] \quad (10)$$

denote the *class- c average density matrix* for the target task, with $\mathcal{A} = \mathcal{T}$, and for the source task, with $\mathcal{A} = \mathcal{S}$. The expected risk (1) for the target task is minimized by the *Hellstrom POVM* $(M_0, I - M_0)$, where M_0 is the projection matrix into the subspace spanned by the eigenvectors of the Hermitian matrix $p_c^{\mathcal{T}}(0)\rho_{\theta,0}^{\mathcal{T}} - p_c^{\mathcal{T}}(1)\rho_{\theta,1}^{\mathcal{T}}$ corresponding to positive eigenvalues [2], with $p_c^{\mathcal{T}}(c)$ denoting the marginal of the joint distribution $p^{\mathcal{T}}(c, x)$. The resulting minimal expected risk for target task can be obtained in closed form as [2]

$$\begin{aligned} \min_{M \in \mathcal{M}} \mathcal{R}_{\theta, M}^{\mathcal{T}} &= \frac{1}{2} - T(p_c^{\mathcal{T}}(0)\rho_{\theta,0}^{\mathcal{T}}, p_c^{\mathcal{T}}(1)\rho_{\theta,1}^{\mathcal{T}}) \\ &= \frac{1}{2} - T^{\mathcal{T}}(\theta), \end{aligned} \quad (11)$$

where the trace distance is defined in (8). In (11), we have defined as $T^{\mathcal{T}}(\theta) = T(p_c^{\mathcal{T}}(0)\rho_{\theta,0}^{\mathcal{T}}, p_c^{\mathcal{T}}(1)\rho_{\theta,1}^{\mathcal{T}})$ the trace distance between the two weighted per-class density matrices for a fixed embedding parameter $\theta \in \Theta$, which we will refer to as the *inter-class trace distance* for the target task under embedding parameter $\theta \in \Theta$. The inter-class trace distance $T^{\mathcal{S}}(\theta)$ for the source task is analogously defined as $T^{\mathcal{S}}(\theta) = T(p_c^{\mathcal{S}}(0)\rho_{\theta,0}^{\mathcal{S}}, p_c^{\mathcal{S}}(1)\rho_{\theta,1}^{\mathcal{S}})$.

By the definition (11), two embedding parameters θ and θ' are similar for task $\mathcal{A} \in \{\mathcal{T}, \mathcal{S}\}$ if the inter-class trace distances $T^{\mathcal{A}}(\theta)$ and $T^{\mathcal{A}}(\theta')$ are close.

Definition 3.1: For task \mathcal{A} , with $\mathcal{A} \in \{\mathcal{S}, \mathcal{T}\}$, the *task-based distance* between any two embedding parameters θ and $\theta' \in \Theta$ is defined as

$$d^{\mathcal{A}}(\theta, \theta') = |T^{\mathcal{A}}(\theta') - T^{\mathcal{A}}(\theta)|, \quad (12)$$

where the inter-class trace distance is defined in (11).

Of particular interest is the task-based distance $d^{\mathcal{A}}(\theta, \theta_*^{\mathcal{A}})$ between any embedding parameter $\theta \in \Theta$ and the embedding parameter $\theta_*^{\mathcal{A}}$ that minimizes the expected risk for task \mathcal{A} , i.e., $\theta_*^{\mathcal{A}} = \arg \min_{\theta \in \Theta} \min_{M \in \mathcal{M}} \mathcal{R}_{M, \theta}^{\mathcal{A}}$, for $\mathcal{A} \in \{\mathcal{S}, \mathcal{T}\}$. If this distance is small, then parameter θ provides a good embedding for task \mathcal{A} . Using this idea, and inspired by [11, Def. 3], we introduce the following definition of task dissimilarity.

Definition 3.2: Tasks \mathcal{T} and \mathcal{S} are D^{ST} -*dissimilar* if we have the inequality

$$d^{\mathcal{T}}(\theta, \theta_*^{\mathcal{T}}) \leq d^{\mathcal{S}}(\theta, \theta_*^{\mathcal{S}}) + D^{ST}. \quad (13)$$

for *all* embedding parameters $\theta \in \Theta$.

Hence, the two tasks are D^{ST} -dissimilar if the suboptimality of each embedding parameter θ on the target task – as measured by the task-based distance to the optimal embedding parameter – differs from the suboptimality for the source task by no more than a parameter D^{ST} . Intuitively, if D^{ST} is small, this should result in a positive transfer of information from source to target task. More precisely, since the task-based distance is never larger than 1 (see Lemma A.1 in

Appendix A), transfer learning is expected to be advantageous only if the relatedness parameter D^{ST} is sufficiently smaller than $\inf_{\theta \in \Theta} 1 - d^S(\theta, \theta_*^S)$.

The following lemma shows that the D^{ST} -dissimilarity of source and target tasks can be expressed in terms of task-based distances.

Lemma 3.1: The target task \mathcal{T} – with optimal embedding parameter $\theta_*^{\mathcal{T}}$ – and the source task \mathcal{S} – with optimal embedding parameter $\theta_*^{\mathcal{S}}$ – are D^{ST} -dissimilar with

$$D^{ST} = \sum_{c \in \{0,1\}} T(p_c^{\mathcal{S}}(c)\rho_{\theta_*^{\mathcal{S}},c}^{\mathcal{S}}, p_c^{\mathcal{T}}(c)\rho_{\theta_*^{\mathcal{T}},c}^{\mathcal{T}}) + \sup_{\theta \in \Theta} (T^{\mathcal{S}}(\theta) - T^{\mathcal{T}}(\theta)). \quad (14)$$

The preceding lemma, whose detailed proof is included in Appendix A, shows that target and source tasks are similar, as per Definition 3.2, if the trace distances between the respective (weighted) per-class density matrices (10) are small, and if the inter-class trace distances are also small for all $\theta \in \Theta$.

C. Main Result

With the background presented in the previous subsections, we are now ready to present our main result in the following theorem.

Theorem 3.1: The following upper bound on transfer excess risk holds with probability at least $1 - \delta$, for $\delta \in (0, 1)$, with respect to the random draw of data sets $\mathcal{D}^{\mathcal{T}}$ and $\mathcal{D}^{\mathcal{S}}$ from the respective joint distributions $p^{\mathcal{T}}(c, x)$ and $p^{\mathcal{S}}(c, x)$,

$$\Delta \mathcal{R}^{\mathcal{S} \rightarrow \mathcal{T}} \leq 2\sqrt{\frac{\mathcal{I}^{\mathcal{T}}}{N^{\mathcal{T}}}} + \sqrt{\frac{\mathcal{I}^{\mathcal{S}}}{N^{\mathcal{S}}}} + 2\mathfrak{R}_{\Theta, \mathcal{M}}^{\mathcal{S}} + D^{ST} + \sqrt{\frac{2}{N^{\mathcal{T}}} \log \frac{3}{\delta}} + \sqrt{\frac{2}{N^{\mathcal{S}}} \log \frac{3}{\delta}} \quad (15)$$

where D^{ST} is the measure of task dissimilarity in (14);

$$\mathfrak{R}_{\Theta, \mathcal{M}}^{\mathcal{S}} = \mathbb{E}_{p^{\mathcal{S}}(c,x) \otimes N^{\mathcal{S}}} \mathbb{E}_{\sigma} \left[\sup_{\theta \in \Theta, M \in \mathcal{M}} \frac{1}{N^{\mathcal{S}}} \sum_{j=1}^{N^{\mathcal{S}}} \sigma_j \ell_{M, \theta}(c_j, x_j) \right] \quad (16)$$

is the source-task Rademacher complexity of the cascade of circuit and measurement with σ denoting an $N^{\mathcal{S}}$ -length vector of Rademacher variables; and

$$\mathcal{I}^{\mathcal{A}} = \sup_{\theta \in \Theta} \left(\text{Tr} \left(\sum_x p^{\mathcal{A}}(x) \rho_{\theta}(x)^2 \right)^{\frac{1}{2}} \right)^2, \quad \text{for } \mathcal{A} \in \{\mathcal{T}, \mathcal{S}\}.$$

The high-probability bound on the transfer excess risk in (15) is a decreasing function of the number of data points $N^{\mathcal{T}}$ and $N^{\mathcal{S}}$ available for the target and source tasks, respectively, and an increasing function of the task dissimilarity measure (14). Furthermore, it increases with the quantities $\mathcal{I}^{\mathcal{T}}$ and $\mathcal{I}^{\mathcal{S}}$, which are measures of correlation between the input x and the quantum embedding $\rho_{\theta}(x)$ under the target and source tasks, respectively. In particular, as we discuss next, the quantities $\mathcal{I}^{\mathcal{T}}$ and $\mathcal{I}^{\mathcal{S}}$ amount to exponential functions of the α -Rényi

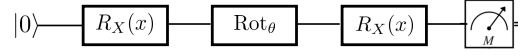


Fig. 2: Embedding circuit for the example in Sec. IV.

MI between the input data x and the quantum representation $\rho_{\theta}(x)$ under the two tasks with $\alpha = 2$.

To illustrate this point, consider a bipartite quantum system comprising of the classical register X reporting the value of input vector x and the quantum register R_{θ} corresponding to the representation $\rho_{\theta}(x)$. For a given embedding parameter vector θ , the *classical-quantum state* of the above bipartite system for task $\mathcal{A} \in \{\mathcal{S}, \mathcal{T}\}$ is described by the density matrix (see, e.g., [4])

$$\rho_{X R_{\theta}}^{\mathcal{A}} = \mathbb{E}_{p^{\mathcal{A}}(x)} [|x\rangle\langle x| \otimes \rho_{\theta}(x)], \quad (17)$$

where \otimes is the Kronecker product, $p^{\mathcal{A}}(x)$ is the marginal of the joint distribution $p^{\mathcal{A}}(c, x)$, and $\{|x\rangle\}$ is an orthonormal basis for the Hilbert space of register X (of dimension equal to the number of possible values for x). As detailed in Section V, the quantities $\mathcal{I}^{\mathcal{T}}$ and $\mathcal{I}^{\mathcal{S}}$ can be seen to equal to $\sup_{\theta \in \Theta} 2^{I_2^{\mathcal{T}}(X; R_{\theta})}$ and $\sup_{\theta \in \Theta} 2^{I_2^{\mathcal{S}}(X; R_{\theta})}$, respectively where $I_2^{\mathcal{A}}(X; R_{\theta})$ is the 2-Rényi MI between the subsystems X and R_{θ} with the density matrix $\rho_{X R_{\theta}}^{\mathcal{A}}$ for task $\mathcal{A} \in \{\mathcal{S}, \mathcal{T}\}$.

IV. EXAMPLE AND DISCUSSION

In this section, we consider a source task and a target task with equiprobable class label $c \in \{0, 1\}$. For each class $c \in \{0, 1\}$, we obtain the discrete-valued input x by quantizing a continuous-valued feature input $\tilde{x} \in \mathbb{R}$ defined as follows. For the source task, the feature \tilde{x} is Gaussian distributed as $\mathcal{N}(\tilde{x} | \mu_c^{\mathcal{S}}, \sigma^2)$ with mean $\mu_c^{\mathcal{S}} \in \mathbb{R}$ and variance σ^2 ; while, for the target task, we have the per-class Gaussian distribution $\mathcal{N}(\tilde{x} | \mu_c^{\mathcal{T}}, \sigma^2)$ with mean $\mu_c^{\mathcal{T}} \in \mathbb{R}$, generally different from that of source task, and the same variance σ^2 . The embedding circuit maps the classical input x to the rank-1 density matrix $\rho_{\theta}(x) = |x\rangle\langle x|$, with the pure quantum state $|x\rangle$ given as

$$|x\rangle = U_{\theta}(x)|0\rangle, \quad \text{with } U_{\theta}(x) = R_X(x)\text{Rot}_{\theta}R_X(x), \quad (18)$$

where $U_{\theta}(x)$ is a unitary matrix parameterized by the angles $\theta = (\theta_1, \theta_2, \theta_3) \in [0, 2\pi]^3$, which constitutes the embedding PQC (see, e.g., [1]). The operation of the embedding circuit is illustrated in Fig. 2, and it involves the Pauli-X rotation $R_X(x)$ (defined as in [1, Eq. (3.45)]) and the general rotation Rot_{θ} defined as in [1, Eq. (3.48)].

In Fig. 3, we plot the transfer excess risk $\Delta \mathcal{R}^{\mathcal{S} \rightarrow \mathcal{T}}$ in (7) (top figure), along with the corresponding upper bound derived in (15) (bottom figure) as a function of the number of target task samples $N^{\mathcal{T}}$ for varying values of source task samples $N^{\mathcal{S}}$. Other parameters are set as $\delta = 0.5$, $\sigma^2 = 0.11$, $\mu_0^{\mathcal{S}} = 1$, $\mu_1^{\mathcal{S}} = -1$, $\mu_0^{\mathcal{T}} = 2.8$, and $\mu_1^{\mathcal{T}} = 0.8$. The transfer excess risk $\Delta \mathcal{R}^{\mathcal{S} \rightarrow \mathcal{T}}$ is a random variable, which is evaluated by drawing multiple pairs of data sets $(\mathcal{D}^{\mathcal{S}}, \mathcal{D}^{\mathcal{T}})$ from their respective joint distributions $p^{\mathcal{S}}(c, x)$ and $p^{\mathcal{T}}(c, x)$. The thick lines in the top figure correspond to the median of the resulting empirical distribution, while the shared areas represent its spread.

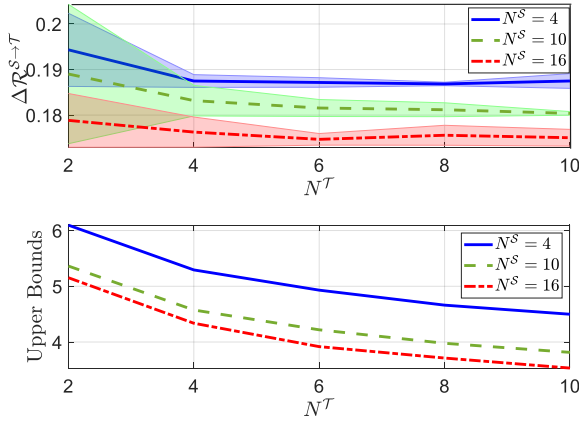


Fig. 3: Transfer excess risk $\Delta\mathcal{R}^{S\rightarrow\mathcal{T}}$ in (7) (top) and upper bound (15) (bottom) as a function of the number of target task samples $N^{\mathcal{T}}$ for varying values of source task samples $N^{\mathcal{S}}$.

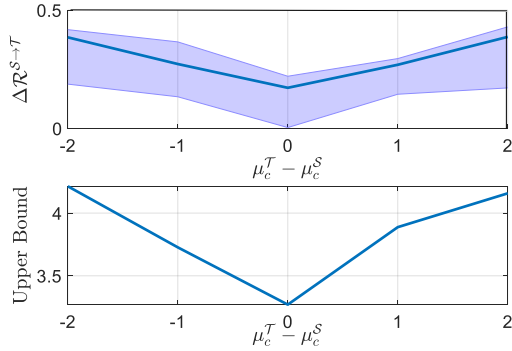


Fig. 4: Transfer excess risk $\Delta\mathcal{R}^{S\rightarrow\mathcal{T}}$ in (7) (top) and upper bound (15) (bottom) as a function of the deviation, $\mu_c^{\mathcal{T}} - \mu_c^{\mathcal{S}}$, of the means of source and target tasks.

The figure shows that the upper bound (15), while numerically loose (as is common for related information-theoretic bounds in classical machine learning [14], [15]), predicts well the relative effect of a change in the number of source and target task samples on the transfer excess risk. In particular, it captures the relative decrease in transfer excess risk when the number $N^{\mathcal{S}}$ of source-task data points are increased, while also reflecting the non-vanishing behavior of the transfer excess risk in the limit of large numbers $N^{\mathcal{T}}$ and $N^{\mathcal{S}}$ of samples from both source and target tasks. As per the bound (15), the residual error can be attributed to the dissimilarity – quantified by D^{ST} – between the source and target tasks.

The impact of the dissimilarity between the two tasks is further elaborated in Fig. 4, which illustrates the transfer excess risk $\Delta\mathcal{R}^{S\rightarrow\mathcal{T}}$ (top) and the corresponding upper bound in (15) (bottom) as a function of the difference $\mu_c^{\mathcal{T}} - \mu_c^{\mathcal{S}}$ between the means of the input data under the target and source tasks for both classes $c \in \{0, 1\}$. We fix $\mu_0^{\mathcal{S}} = 1$, $\mu_1^{\mathcal{S}} = -2$, $N^{\mathcal{T}} = 4$, $N^{\mathcal{S}} = 10$, $\sigma^2 = 1$, and $\delta = 0.9$. As can be seen, when the difference between the means is zero, i.e., when the source and target tasks coincide, the transfer excess risk, and the corresponding upper bound, are minimized. Conversely, when the mean of the target task

deviates from that of the source task, the transfer excess risk increases, as correctly predicted by the upper bound.

V. PROOF OF THEOREM 3.1

To derive the upper bound in Theorem 3.1, we make use of the following auxiliary lemma, the proof of which is in Appendix B. To this end, for fixed $\theta \in \Theta$, we define $M_{\theta}^{\mathcal{A}} = \arg \min_{M \in \mathcal{M}} \mathcal{R}_{\theta, M}^{\mathcal{A}}$ and $\widehat{M}_{\theta}^{\mathcal{A}} = \arg \min_{M \in \mathcal{M}} \widehat{\mathcal{R}}_{\theta, M}^{\mathcal{A}}$ as the optimal measurements minimizing the expected risk and the empirical training loss respectively, of task $\mathcal{A} \in \{\mathcal{S}, \mathcal{T}\}$.

Lemma 5.1: The following upper bound on the transfer excess risk holds for D^{ST} -related source and target tasks,

$$\Delta\mathcal{R}^{S\rightarrow\mathcal{T}} \leq 2\mathcal{G}_{\theta}^{\mathcal{T}}(\mathcal{D}^{\mathcal{T}}) + d^{\mathcal{S}}(\hat{\theta}, \theta_*^{\mathcal{T}}) + D^{ST} \quad (19)$$

$$\leq 2\mathcal{G}_{\theta}^{\mathcal{T}}(\mathcal{D}^{\mathcal{T}}) + \mathcal{G}^{\mathcal{S}}(\mathcal{D}^{\mathcal{S}}) + \mathcal{G}_{\theta_*^{\mathcal{S}}}^{\mathcal{S}}(\mathcal{D}^{\mathcal{S}}) + D^{ST}, \quad (20)$$

where $\mathcal{G}_{\theta}^{\mathcal{A}}(\mathcal{D}^{\mathcal{A}}) = \sup_{M \in \mathcal{M}} |\mathcal{R}_{\theta, M}^{\mathcal{A}} - \widehat{\mathcal{R}}_{\theta, M}^{\mathcal{A}}|$ denotes the generalization error for a fixed embedding parameter $\theta \in \Theta$ and $\mathcal{G}^{\mathcal{A}}(\mathcal{D}^{\mathcal{A}}) = \sup_{\theta \in \Theta} \mathcal{G}_{\theta}^{\mathcal{A}}(\mathcal{D}^{\mathcal{A}})$ denotes the supremum of generalization error $\mathcal{G}_{\theta}^{\mathcal{A}}(\mathcal{D}^{\mathcal{A}})$ over $\theta \in \Theta$ for task \mathcal{A} .

We are now ready to state the proof of Theorem 3.1. The idea is to bound each of the first three terms in the upper bound (20) with high probability with respect to the training data sets, and then combine the resulting bounds via the union bound. Noting that the loss function $\ell_{M, \theta}(c, x)$ in (2) is $[0, 1]$ -bounded, the classical Rademacher complexity-based generalization bound [16] gives that with probability at least $1 - \delta'$ over the random draw of data $\mathcal{D}^{\mathcal{A}} \sim p^{\mathcal{A}}(c, x)^{\otimes N^{\mathcal{A}}}$, for $\mathcal{A} \in \{\mathcal{S}, \mathcal{T}\}$, the following inequality holds

$$\mathcal{G}_{\theta}^{\mathcal{A}}(\mathcal{D}^{\mathcal{A}}) \leq 2\mathfrak{R}_{\theta}^{\mathcal{A}}(\mathcal{M}) + \sqrt{\frac{1}{2N^{\mathcal{A}}} \log\left(\frac{1}{\delta'}\right)} \quad (21)$$

$$\leq 2 \sup_{\theta \in \Theta} \mathfrak{R}_{\theta}^{\mathcal{A}}(\mathcal{M}) + \sqrt{\frac{1}{2N^{\mathcal{A}}} \log\left(\frac{1}{\delta'}\right)}, \quad (22)$$

where $\mathfrak{R}_{\theta}^{\mathcal{A}}(\mathcal{M}) = \mathbb{E}_{p^{\mathcal{A}}(c, x)^{\otimes N^{\mathcal{A}}}} \mathbb{E}_{\sigma} \left[\sup_{M \in \mathcal{M}} \frac{1}{N^{\mathcal{A}}} \sum_{j=1}^{N^{\mathcal{A}}} \sigma_j \ell_{M, \theta}(c_j, x_j) \right]$ is the Rademacher complexity of the space \mathcal{M} of the POVM for fixed θ , with $\sigma = (\sigma_1, \dots, \sigma_{N^{\mathcal{A}}})$ denoting a vector of i.i.d. Rademacher random variables. It then follows from [3, Thm. 2] that for binary classification with fixed $\theta \in \Theta$, we have

$$\mathfrak{R}_{\theta}^{\mathcal{A}}(\mathcal{M}) \leq \frac{1}{2\sqrt{N^{\mathcal{A}}}} \text{Tr} \left(\sum_x p^{\mathcal{A}}(x) \rho_{\theta}(x)^2 \right)^{\frac{1}{2}} = \frac{1}{2} \sqrt{\frac{2I_2^{\mathcal{A}}(X; R_{\theta})}{N^{\mathcal{A}}}} \quad (23)$$

where $I_2^{\mathcal{A}}(X; R_{\theta})$ is the 2-Rényi MI between subsystems X and R_{θ} of task \mathcal{A} for fixed $\theta \in \Theta$. Using (23) in (22) gives a high probability bound on $\mathcal{G}_{\theta}^{\mathcal{A}}(\mathcal{D}^{\mathcal{A}})$ which holds with probability at least $1 - \delta'$ for task \mathcal{A} and $\theta \in \Theta$. The second term in (20) can be bounded, with probability at least $1 - \tilde{\delta}$, as [16] $\mathcal{G}^{\mathcal{S}}(\mathcal{D}^{\mathcal{S}}) \leq 2\mathfrak{R}_{\Theta, \mathcal{M}}^{\mathcal{S}} + \sqrt{\frac{1}{2N^{\mathcal{S}}} \log\left(\frac{1}{\tilde{\delta}}\right)}$ where $\mathfrak{R}_{\Theta, \mathcal{M}}^{\mathcal{S}}$ is defined as in (16). Combining the above bound on the second term of (20) with those on the first and third terms, adopted by using (23) in (22), via union bound gives the required upper bound with the choice of $\delta' = \tilde{\delta} = \delta/3$.

VI. CONCLUSIONS

This paper studies the generalization performance of quantum binary classifiers in which quantum embedding is pre-trained based on data from a source task that is distinct from the target task of interest. The main result of this paper is an information-theoretic high-probability bound on the transfer excess risk that depends on the correlation between quantum embedding and classical input, as measured by Rényi MI, as well as on the (dis)similarity between source and target tasks.

APPENDIX A PROOF OF LEMMA 3.1

As a useful auxiliary result to prove Lemma 3.1, we first state and prove the following lemma.

Lemma A.1: For $\mathcal{A} \in \{\mathcal{S}, \mathcal{T}\}$, the following inequalities hold for all $\theta \in \Theta$:

$$0 \leq d^{\mathcal{A}}(\theta, \theta_*^{\mathcal{A}}) = T^{\mathcal{A}}(\theta_*^{\mathcal{A}}) - T^{\mathcal{A}}(\theta) \quad (24)$$

$$\leq T\left(p_c^{\mathcal{A}}(0)(\rho_{\theta_*^{\mathcal{A}},0}^{\mathcal{A}} - \rho_{\theta,0}^{\mathcal{A}}), p_c^{\mathcal{A}}(1)(\rho_{\theta_*^{\mathcal{A}},1}^{\mathcal{A}} - \rho_{\theta,1}^{\mathcal{A}})\right) \leq 1. \quad (25)$$

Proof: The equality in (24) follows from the definition of task-based distance in Definition 3.1 as

$$d^{\mathcal{A}}(\theta, \theta_*^{\mathcal{A}}) = |0.5 + T^{\mathcal{A}}(\theta_*^{\mathcal{A}}) - 0.5 - T^{\mathcal{A}}(\theta)| \quad (26a)$$

$$= \left| \min_{M \in \mathcal{M}} \mathcal{R}_{\theta, M}^{\mathcal{T}} - \min_{M \in \mathcal{M}} \mathcal{R}_{\theta_*^{\mathcal{A}}, M}^{\mathcal{T}} \right| \quad (26b)$$

$$= \min_{M \in \mathcal{M}} \mathcal{R}_{\theta, M}^{\mathcal{T}} - \min_{M \in \mathcal{M}} \mathcal{R}_{\theta_*^{\mathcal{A}}, M}^{\mathcal{T}} \quad (26c)$$

$$= T^{\mathcal{A}}(\theta_*^{\mathcal{A}}) - T^{\mathcal{A}}(\theta), \quad (26d)$$

where (26b) is an application of (11); (26c) follows from the definition of $\theta_*^{\mathcal{A}}$ and (26d) follows again from (11). The upper bound in (25) is a consequence of the variational representation of trace distance [4]. To see this, let $\sigma(\theta_*^{\mathcal{A}}) = p_c^{\mathcal{A}}(0)\rho_{\theta_*^{\mathcal{A}},0}^{\mathcal{A}} - p_c^{\mathcal{A}}(1)\rho_{\theta_*^{\mathcal{A}},1}^{\mathcal{A}}$ and $\sigma(\theta) = p_c^{\mathcal{A}}(0)\rho_{\theta,0}^{\mathcal{A}} - p_c^{\mathcal{A}}(1)\rho_{\theta,1}^{\mathcal{A}}$. We then have the following sequence of relations

$$T^{\mathcal{A}}(\theta_*^{\mathcal{A}}) - T^{\mathcal{A}}(\theta) \quad (27a)$$

$$\stackrel{(a)}{=} \max_{0 \leq \Lambda \leq I} \text{Tr}(\Lambda \sigma(\theta_*^{\mathcal{A}})) - \max_{0 \leq \Lambda \leq I} \text{Tr}(\Lambda \sigma(\theta)) \quad (27b)$$

$$\leq \max_{0 \leq \Lambda \leq I} \text{Tr}(\Lambda (\sigma(\theta_*^{\mathcal{A}}) - \sigma(\theta))) \quad (27c)$$

$$\stackrel{(b)}{=} T\left(p_c^{\mathcal{A}}(0)(\rho_{\theta_*^{\mathcal{A}},0}^{\mathcal{A}} - \rho_{\theta,0}^{\mathcal{A}}), p_c^{\mathcal{A}}(1)(\rho_{\theta_*^{\mathcal{A}},1}^{\mathcal{A}} - \rho_{\theta,1}^{\mathcal{A}})\right), \quad (27d)$$

where (a) and (b) follow from the variational characterization of trace distance [4, Lem. 9.1.1], where the maximization is over all positive semi-definite matrices Λ whose eigenvalues are upper bounded by 1. ■

Using Lemma A.1, Lemma 3.1 follows as

$$d^{\mathcal{T}}(\hat{\theta}, \theta_*^{\mathcal{T}}) \stackrel{(a)}{=} T^{\mathcal{T}}(\theta_*^{\mathcal{T}}) - T^{\mathcal{T}}(\hat{\theta}) \quad (28a)$$

$$= T(p_c^{\mathcal{T}}(0)\rho_{\hat{\theta},0}^{\mathcal{T}}, p_c^{\mathcal{T}}(1)\rho_{\hat{\theta},1}^{\mathcal{T}}) - T^{\mathcal{T}}(\hat{\theta}) \quad (28b)$$

$$\stackrel{(b)}{\leq} T(p_c^{\mathcal{T}}(0)\rho_{\hat{\theta},0}^{\mathcal{T}}, p_c^{\mathcal{S}}(0)\rho_{\theta_*^{\mathcal{S}},0}^{\mathcal{S}}) + T(p_c^{\mathcal{S}}(0)\rho_{\theta_*^{\mathcal{S}},0}^{\mathcal{S}}, p_c^{\mathcal{S}}(1)\rho_{\theta_*^{\mathcal{S}},1}^{\mathcal{S}}) \\ + T(p_c^{\mathcal{S}}(1)\rho_{\theta_*^{\mathcal{S}},1}^{\mathcal{S}}, p_c^{\mathcal{T}}(1)\rho_{\hat{\theta},1}^{\mathcal{T}}) - T^{\mathcal{T}}(\hat{\theta}) + T^{\mathcal{S}}(\hat{\theta}) - T^{\mathcal{S}}(\hat{\theta}) \quad (28c)$$

$$= d^{\mathcal{S}}(\hat{\theta}, \theta_*^{\mathcal{S}}) + \sum_{c \in \{0,1\}} T(p_c^{\mathcal{S}}(c)\rho_{\theta_*^{\mathcal{S}},c}^{\mathcal{S}}, p_c^{\mathcal{T}}(c)\rho_{\hat{\theta},c}^{\mathcal{T}}) \\ + T^{\mathcal{S}}(\hat{\theta}) - T^{\mathcal{T}}(\hat{\theta}) \quad (28d)$$

$$\leq d^{\mathcal{S}}(\hat{\theta}, \theta_*^{\mathcal{S}}) + D^{ST}, \quad (28e)$$

where the equality in (a) is an application of Lemma A.1, and the inequality in (b) follows from the triangle inequality property of the trace distance [4].

APPENDIX B PROOF OF LEMMA 5.1

Recall that $M_{\theta}^{\mathcal{A}} = \arg \min_{M \in \mathcal{M}} \mathcal{R}_{\theta, M}^{\mathcal{A}}$ denotes the optimal measurement minimizing the expected risk of task $\mathcal{A} \in \{\mathcal{S}, \mathcal{T}\}$ for fixed $\theta \in \Theta$. Analogously, for fixed $\theta \in \Theta$, $\widehat{M}_{\theta}^{\mathcal{A}} = \arg \min_{M \in \mathcal{M}} \widehat{\mathcal{R}}_{\theta, M}^{\mathcal{A}}$ denotes the optimal measurement minimizing the empirical training loss of task $\mathcal{A} \in \{\mathcal{S}, \mathcal{T}\}$.

To obtain the upper bound in (19), we start by decomposing the transfer excess risk as

$$\Delta \mathcal{R}^{\mathcal{S} \rightarrow \mathcal{T}} = \underbrace{\mathcal{R}_{\hat{\theta}, \widehat{M}_{\hat{\theta}}^{\mathcal{T}}}^{\mathcal{T}} - \mathcal{R}_{\hat{\theta}, M_{\hat{\theta}}^{\mathcal{T}}}^{\mathcal{T}}}_{\mathcal{E}_{\mathcal{T}}(\hat{\theta})} + \mathcal{R}_{\hat{\theta}, M_{\hat{\theta}}^{\mathcal{T}}}^{\mathcal{T}} - \mathcal{R}_{\theta_*^{\mathcal{T}}, M_{\theta_*^{\mathcal{T}}}^{\mathcal{T}}} \quad (29a)$$

$$\stackrel{(a)}{\leq} 2\mathcal{G}_{\hat{\theta}}^{\mathcal{T}}(\mathcal{D}^{\mathcal{T}}) + \mathcal{R}_{\hat{\theta}, M_{\hat{\theta}}^{\mathcal{T}}}^{\mathcal{T}} - \mathcal{R}_{\theta_*^{\mathcal{T}}, M_{\theta_*^{\mathcal{T}}}^{\mathcal{T}}} \quad (29b)$$

$$= 2\mathcal{G}_{\hat{\theta}}^{\mathcal{T}}(\mathcal{D}^{\mathcal{T}}) + d^{\mathcal{T}}(\hat{\theta}, \theta_*^{\mathcal{T}}) \quad (29c)$$

where the upper bound in (a) follows by a canonical decomposition of $\mathcal{E}_{\mathcal{T}}(\hat{\theta})$ as follows:

$$\mathcal{E}_{\mathcal{T}}(\hat{\theta}) = \mathcal{R}_{\hat{\theta}, \widehat{M}_{\hat{\theta}}^{\mathcal{T}}}^{\mathcal{T}} - \widehat{\mathcal{R}}_{\hat{\theta}, \widehat{M}_{\hat{\theta}}^{\mathcal{T}}}^{\mathcal{T}} + \underbrace{\widehat{\mathcal{R}}_{\hat{\theta}, \widehat{M}_{\hat{\theta}}^{\mathcal{T}}}^{\mathcal{T}} - \widehat{\mathcal{R}}_{\hat{\theta}, M_{\hat{\theta}}^{\mathcal{T}}}^{\mathcal{T}}}_{\leq 0} + \widehat{\mathcal{R}}_{\hat{\theta}, M_{\hat{\theta}}^{\mathcal{T}}}^{\mathcal{T}} - \mathcal{R}_{\hat{\theta}, M_{\hat{\theta}}^{\mathcal{T}}}^{\mathcal{T}} \\ \leq \mathcal{R}_{\hat{\theta}, \widehat{M}_{\hat{\theta}}^{\mathcal{T}}}^{\mathcal{T}} - \widehat{\mathcal{R}}_{\hat{\theta}, \widehat{M}_{\hat{\theta}}^{\mathcal{T}}}^{\mathcal{T}} + \widehat{\mathcal{R}}_{\hat{\theta}, M_{\hat{\theta}}^{\mathcal{T}}}^{\mathcal{T}} - \mathcal{R}_{\hat{\theta}, M_{\hat{\theta}}^{\mathcal{T}}}^{\mathcal{T}} \leq 2\mathcal{G}_{\hat{\theta}}^{\mathcal{T}}(\mathcal{D}^{\mathcal{T}}). \quad (30)$$

The bound in (19) then follows from the inequality in (29c) using the definition of D^{ST} -related tasks in Definition 3.2.

We now prove the upper bound in (20), which is obtained by further upper bounding the source task-distance $d^{\mathcal{S}}(\hat{\theta}, \theta_*^{\mathcal{S}})$

in (19). Towards this, we have the following sequence of inequalities

$$d^S(\hat{\theta}, \theta_*^S) = \mathcal{R}_{\hat{\theta}, M_{\hat{\theta}}^S}^S - \mathcal{R}_{\theta_*^S, M_{\theta_*^S}^S}^S \quad (31a)$$

$$\stackrel{(a)}{\leq} \mathcal{R}_{\hat{\theta}, \widehat{M}_{\hat{\theta}}^S}^S - \mathcal{R}_{\theta_*^S, M_{\theta_*^S}^S}^S \quad (31b)$$

$$= \mathcal{R}_{\hat{\theta}, \widehat{M}_{\hat{\theta}}^S}^S - \widehat{\mathcal{R}}_{\hat{\theta}, \widehat{M}_{\hat{\theta}}^S}^S + \widehat{\mathcal{R}}_{\hat{\theta}, \widehat{M}_{\hat{\theta}}^S}^S - \widehat{\mathcal{R}}_{\theta_*^S, M_{\theta_*^S}^S}^S \\ + \widehat{\mathcal{R}}_{\theta_*^S, M_{\theta_*^S}^S}^S - \mathcal{R}_{\theta_*^S, M_{\theta_*^S}^S}^S \quad (31c)$$

$$\stackrel{(b)}{\leq} \mathcal{R}_{\hat{\theta}, \widehat{M}_{\hat{\theta}}^S}^S - \widehat{\mathcal{R}}_{\hat{\theta}, \widehat{M}_{\hat{\theta}}^S}^S + \widehat{\mathcal{R}}_{\theta_*^S, M_{\theta_*^S}^S}^S - \mathcal{R}_{\theta_*^S, M_{\theta_*^S}^S}^S \quad (31d)$$

$$\leq \mathcal{G}_{\hat{\theta}}^S(\mathcal{D}^S) + \mathcal{G}_{\theta_*^S}^S(\mathcal{D}^S), \quad (31e)$$

where the inequality in (a) follows since for fixed $\hat{\theta}$, $M_{\hat{\theta}}^S$ optimizes the expected risk $\mathcal{R}_{M, \hat{\theta}}^S$, and the inequality in (b) similarly follows since $\hat{\theta}$ minimizes the training loss $\min_{M \in \mathcal{M}} \widehat{\mathcal{R}}_{M, \hat{\theta}}^S$, whereby $\widehat{\mathcal{R}}_{\hat{\theta}, \widehat{M}_{\hat{\theta}}^S}^S - \widehat{\mathcal{R}}_{\theta_*^S, M_{\theta_*^S}^S}^S \leq 0$. Combining (31e) with the upper bound in (19) yields (20).

APPENDIX C DETAILS OF EXAMPLE

For the example considered in Section IV, the Pauli-X rotation is defined as

$$R_X(x) = \begin{bmatrix} \cos(x/2) & -i \sin(x/2) \\ i \sin(x/2) & \cos(x/2) \end{bmatrix}, \quad (32)$$

and the general rotation Rot_{θ} is defined as

$$\text{Rot}_{\theta} = \begin{bmatrix} e^{i(-\frac{\theta_1}{2} - \frac{\theta_3}{2})} \cos(\theta_2/2) & -e^{i(-\frac{\theta_1}{2} + \frac{\theta_3}{2})} \sin(\theta_2/2) \\ e^{i(\frac{\theta_1}{2} - \frac{\theta_3}{2})} \sin(\theta_2/2) & e^{i(\frac{\theta_1}{2} + \frac{\theta_3}{2})} \cos(\theta_2/2) \end{bmatrix}.$$

REFERENCES

- [1] M. Schuld and F. Petruccione, *Machine Learning with Quantum Computers*. Springer Nature, 2021.
- [2] C. W. Helstrom, “Quantum detection and estimation theory,” *Journal of Statistical Physics*, vol. 1, no. 2, pp. 231–252, 1969.
- [3] L. Banchi, J. Pereira, and S. Pirandola, “Generalization in quantum machine learning: A quantum information standpoint,” *Quantum*, vol. 2, no. 4, p. 040321, 2021.
- [4] M. M. Wilde, *Quantum information theory*. Cambridge University Press, 2013.
- [5] A. Mari, T. R. Bromley, J. Izaac, M. Schuld, and N. Killoran, “Transfer learning in hybrid classical-quantum neural networks,” *Quantum*, vol. 4, p. 340, 2020.
- [6] M. C. Caro, E. Gil-Fuster, J. J. Meyer, J. Eisert, and R. Sweke, “Encoding-dependent generalization bounds for parametrized quantum circuits,” *Quantum*, vol. 5, p. 582, 2021.
- [7] K. Bu, D. E. Koh, L. Li, Q. Luo, and Y. Zhang, “Rademacher complexity of noisy quantum circuits,” *arXiv preprint arXiv:2103.03139*, 2021.
- [8] —, “On the statistical complexity of quantum circuits,” *arXiv preprint arXiv:2101.06154*, 2021.
- [9] H.-Y. Huang, M. Broughton, J. Cotler, S. Chen, J. Li, M. Mohseni, H. Neven, R. Babbush, R. Kueng, J. Preskill, and J. R. McClean, “Quantum advantage in learning from experiments,” *arXiv preprint arXiv:2112.00778*, 2021.
- [10] A. Abbas, D. Sutter, C. Zoufal, A. Lucchi, A. Figalli, and S. Woerner, “The power of quantum neural networks,” *Nature Computational Science*, vol. 1, no. 6, pp. 403–409, 2021.
- [11] N. Tripuraneni, M. I. Jordan, and C. Jin, “On the theory of transfer learning: The importance of task diversity,” *arXiv preprint arXiv:2006.11650*, 2020.
- [12] J. Watrous, *The theory of quantum information*. Cambridge University Press, 2018.
- [13] M. Berta, K. P. Seshadreesan, and M. M. Wilde, “Rényi generalizations of the conditional quantum mutual information,” *Journal of Mathematical Physics*, vol. 56, no. 2, p. 022205, 2015.
- [14] X. Wu, J. H. Manton, U. Aickelin, and J. Zhu, “Information-theoretic analysis for transfer learning,” in *2020 IEEE International Symposium on Information Theory (ISIT)*, pp. 2819–2824.
- [15] S. T. Jose and O. Simeone, “Information-theoretic bounds on transfer generalization gap based on jensen-shannon divergence,” in *2021 29th European Signal Processing Conference (EUSIPCO)*, pp. 1461–1465.
- [16] S. Shalev-Shwartz and S. Ben-David, *Understanding machine learning: From theory to algorithms*. Cambridge University Press, 2014.